Chemical Physics Letters 599 (2014) 154–158

Contents lists available at ScienceDirect

Chemical Physics Letters

journal homepage: www.elsevier.com/locate/cplett

Reduced thermal conductivity of isotope substituted carbon nanomaterials: Nanotube versus graphene nanoribbon

Upamanyu Ray, Ganesh Balasubramanian *

Department of Mechanical Engineering, Iowa State University, Ames, IA 50011, USA

ARTICLE INFO

Article history:
Received 31 January 2014
In final form 13 March 2014
Available online 20 March 2014

ABSTRACT

Non-equilibrium molecular dynamics (MD) simulations of isotopically impure carbon nanotubes (CNTs) and graphene nanoribbons (GNRs) of varying lengths reveal that the relative decrease in thermal conductivity (k) in both the nanostructures are similar for constant isotope substitution. We find that the delocalized transverse modes in CNTs and the out-of-plane flexural modes in GNRs exert a substantial contribution to the thermal transport whereas the influence of isotope substitution on the phonon density of states (DOS) is similar in all directions. The vibrational spectra for different length scales consistently show that the energy modes shift to lower wave numbers reflecting the strong influence of mass disorder that reduces the energy transport through these nanomaterials, consequently lowering k.

1. Introduction

Carbon nanomaterials have received widespread interest since their discovery [1] because of their unique mechanical, thermal and electrical properties. However, ambiguity exists about the differences in the fundamental physics governing heat transfer through 1D (or semi-1D as some previous literature [2,3] suggest but since that does not influence our analysis, we refer to carbon nanotubes or CNTs as a 1D material throughout) and 2D (graphene nanoribbons or GNRs) [4,5] forms of carbon nanomaterials. For instance, there is disagreement in the literature about the dominant phonon (lattice vibration) modes that contribute to the thermal transport through them [6,7]. This could become more significant in presence of mass disorder created by isotope or vacancy defects in these nanomaterials which have been observed from theoretical as well as experimental studies in these nanomaterials [8–11]. Thus, comparing the heat conduction mechanisms in CNTs and GNRs [12,13] would facilitate design of novel carbon nanomaterials and prediction of their transport characteristics geared towards targeted applications in electronics, thermoelectrics etc. [14–18].

Earlier investigations suggest that for graphene the in-plane vibrational modes along the direction of heat transfer mainly influence the thermal transport while other efforts propose that the out-of plane low energy flexural vibrational modes exert the dominant effect on the heat transfer [6]. Here, we employ classical molecular simulations to explore contributions of the various vibrational modes in the heat transfer through these carbon nanostructures, with and without isotope substitution. Our study provides insinuations about the decrease in k with mass disorder induced by the presence of isotopes and investigates whether mass impurities influence the dominant or non-dominant modes or both, causing impedance to heat transfer.

Reports that describe the role of isotope substitution on thermal conductivity for varying material dimensions are sparse. We present our findings for reduction in k with constant isotope (^{14}C) substitution in both CNT and GNR with varying material lengths, and infer that the relative thermal conductivity decrease for isotope substituted nanomaterials relative to the pure forms remains invariant to changes in the characteristic dimension. The contribution of the mass disorder to both the dominant and the non-dominant vibrational modes are described.

2. Methodology

We employ MD simulations to examine armchair (10, 10) CNTs and GNRs with lengths (x-direction) ranging from 20 to 110 nm with varying number of carbon atoms, as listed in Table 1. As the literature [19,20] suggests that k is strongly dependent on the thickness of GNRs and the diameter and chirality of CNTs, these parameters are kept invariant in our investigations. The CNTs are made by zone-folding approach from GNRs of similar lengths and 4.26 nm width (y-direction). The thickness of the GNR sheet is the Van der Waals diameter of a carbon atom, 0.34 nm [21]. We select 10% of the carbon (^{12}C) atoms randomly and substitute them by the heavier ^{14}C isotope. Each structure is initialized at a temperature of 300 K and pressure of approximately 1 bar. Periodic

* Corresponding author. Address: Department of Mechanical Engineering, 2092 Black Engineering, Iowa State University, Ames, IA 50011, USA.
E-mail address: bganesh@iastate.edu (G. Balasubramanian).

http://dx.doi.org/10.1016/j.cplett.2014.03.038
0009-2614/

Table 1
The length (L) of the nanostructures (CNT and GNR) and number of carbon atoms contained in them are listed. The corresponding simulation box dimensions are $L(x) \times 4.26$ nm$(y) \times 10.4$ nm(z) for GNRs and $L(x) \times 10.4$ nm$(y) \times 10.4$ nm(z) for CNTs. The numbers of atoms involved in the energy exchange for thermal conductivity calculations are also listed.

Length of GNRs/CNTs (nm)	20	35	50	65	80	95	110
Number of atoms	3280	5720	8160	10600	13040	14680	17920
Total number of atoms in the two cold slabs at the nanomaterial boundaries	66	120	160	240	253	330	360
Total number of atoms in the hot slab at the center of the nanomaterial	66	120	160	240	253	330	360

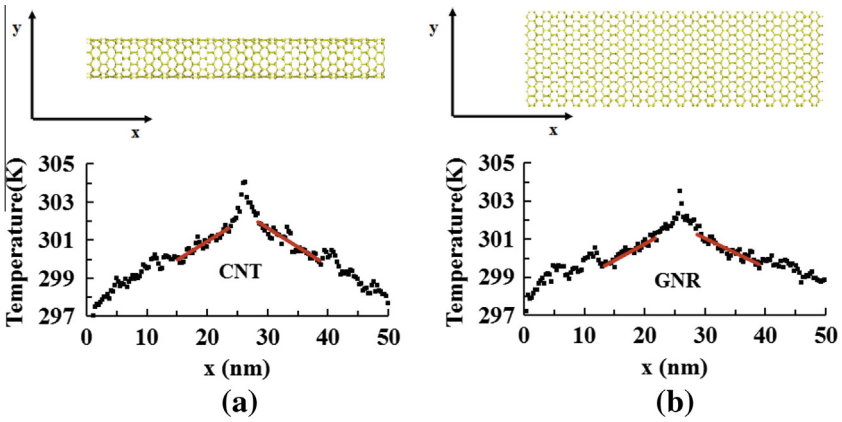

Figure 1. The steady-state temperature distribution along the direction of heat transfer obtained from the MD simulations are presented for (a) CNT and (b) GNR, each of length $L = 50$ nm.

boundary conditions (PBCs) are imposed in all directions with the y- and z-axes dimensions of the simulation cell large enough to prevent the structures from interacting with their own periodic images. We employ the 3-body Tersoff potential that models the attractive and repulsive bonded as well as the non-bonded interactions in both CNTs and GNRs, and is known to provide robust predictions [22–26]. The highly parallelized LAMMPS package [27] is used for all our simulations.

We perform equilibrium MD simulations with isothermal–isobaric ensemble (NPT) under the Nóse–Hoover thermostat and barostat (each with a coupling time of 0.1 ps) followed by canonical (NVT) simulations, each for 7 ns. Subsequently, simulations under the microcanonical ensemble (NVE) are employed for a further 2 ns to equilibrate the system in absence of imposed constraints. A timestep of 0.001 ps is used throughout in all the simulations. The results are obtained under the ergodic hypothesis assumption employing a time average for the computed data in lieu of an ensemble sampling [28].

We calculate the phonon density of states (DOS) from the Fourier transform of the averaged mass-weighted velocity autocorrelation function (VACF). We continue the equilibrium simulations for additional 1 ns recording the trajectories of the equilibrated nanostructures after every 100 ps. Each of these are again simulated for an additional 8.5 ps where the velocities, recorded after every 1 fs, are used to compute the time-translation invariance of the VACF with a correlation time of 8.192 ps and averaging over 309 time origins. The overall average of all the VACFs is Fourier transformed to obtain the desired phonon DOS spectra with a resolution of 2.036 cm^{-1}. The heat transfer is along the x-wise direction for both CNTs and GNRs. For the nanotubes both y- and z-axes are the transverse directions, while the z-axis represents the out-of-plane direction for the 2D GNRs.

We apply the reverse non-equilibrium MD (RNEMD [29,30] approach to compute the thermal conductivities for the different GNRs and CNTs along the in-plane x direction using the canonical (NVT) ensemble for 8 ns. Each of the structures are partitioned into 100 bins (or 'slabs') along the x-direction. In the present research, the number of slabs is constant for all lengths of the nanomaterials and equal to 100. Hence the size of each slab increases with increasing lengths of the nanostructures and the number of atoms involved in the energy exchange process is provided in Table 1. Employing a kinetic energy exchange mechanism, the central bins are artificially heated while the ones at the boundaries are cooled. Around 280 atoms from the cool boundaries and the same number from the hot slab at the center get involved in this energy exchange. This drives a heat transfer process through the nanomaterial. A steady state temperature distribution is achieved after 7 ns which is used to calculate the heat flux through the material and the temperature gradient. We continue the simulations for additional 1 ns to compute the average energy transferred and the spatially distributed temperature values. Figure 1a and b respectively show the spatial temperature distribution for pure CNT and GNR of length 50 nm. We find the temperature distributions are linear and symmetric about the mid-plane of the nanostructures [21,30]. Given the linear variation of temperature, we employ the empirical Fourier's Law to compute k. We obtain $k = [\Sigma(m/2)(V_h^2 - V_c^2)]/(2t\,A\,dT/dx)$, where $\Sigma(m/2)(V_h^2 - V_c^2)$ provides the kinetic energy exchanged within the simulated structure, t is the simulation time, A is the cross-sectional area across which heat transfer occurs and dT/dx is the temperature gradient. Disagreements exist in the determination of the cross-section, especially for CNTs [31–33]. We use the Van der Waals diameter of each carbon atom as the thickness of the nanotube or nanoribbbon throughout our analysis. For nanotube the cross-sectional area is that of a concentric cylinder with its thickness being the diameter of a carbon atom. On the other hand, for the nanoribbons, the cross-section is simply the rectangular area with the width (y-axis) of GNR (4.26 nm) and thickness equal to the diameter of the carbon atom.

3. Results and discussion

The length dependence of k for both pure and isotopically impure CNTs and GNRs are presented in Figure 2a and b. k varies from 101.2725 $Wm^{-1}\,K^{-1}$ for 20 nm pure CNT to 345.706 $Wm^{-1}\,K^{-1}$ for 110 nm pure CNT while the corresponding pure GNRs have $k = 86.34$ $Wm^{-1}\,K^{-1}$ and 215.5 $Wm^{-1}\,K^{-1}$ respectively. The increase in k with increasing length agrees well with earlier